Statistical Analysis of the Effects of Aluminum Oxide (Al_2O_3) Nanoparticle, TBAC, and APG on Storage Capacity of CO_2 Hydrate Formation

Bozorgian, Ali Reza; Arab Aboosadi, Zahra*[+]

Department of Chemical Engineering, Marvdasht Branch, Islamic Azad University, Marvdasht, I.R. IRAN

Mohammadi, Abolfazl

Department of Chemical Engineering, University of Bojnord, Bojnord, I.R. IRAN

Honarvar, Bizhan

Department of Chemical Engineering, Marvdasht Branch, Islamic Azad University, Marvdasht, I.R. IRAN

Azimi, Ali Reza

Department of Chemical Engineering, Mahshahr Branch, Islamic Azad University, Mahshahr, I.R. IRAN

ABSTRACT: *In this study, the effect of various concentrations of alkyl polyglycoside (APG), aluminum oxide nanoparticles (Al_2O_3), and tetra-n-butyl ammonium chloride (TBAC) on the storage capacity of CO_2 hydrate formation are investigated. For this aim, a laboratory system is developed. The experiments are carried out in the pressure range of 25 to 35 bar and the temperature range of 275.15 K to 279.15 K. The Experimental results showed that by increasing the system pressure at a constant temperature, the storage capacity increased by 48% on average. Decreasing the system temperature at constant pressure increased the storage capacity by 23% on average. Adding APG to the system at constant temperature and pressure increases the storage capacity by 75% on average, while adding nanoparticles of aluminum oxide increases the storage capacity by 5% and TBAC 38% on average. For statistical analysis of laboratory data, Design-Expert software and Response Surface test design method, and Quadratic model are employed and a mathematical relationship is developed with R^2 = 0.9987 to estimate CO_2 storage capacity in hydrates. The optimum amount of storage capacity equal to 137.476 has been reached at 34.558 bar, 276.085 K, 2.825 wt% of TBAC, 956.733 ppm APG, 2.436 wt % Al_2O_3.*

KEYWORDS: *Gas hydrates; Storage capacity; Aluminum oxide nanoparticle; APG; Statistical analysis.*

* *To whom correspondence should be addressed.*

+ E-mail: aboosadi@miau.ac.ir

1021-9986/2022/1/220-231 12/$/6.02

INTRODUCTION

Carbon dioxide is one of the most effective greenhouse gases in global warming and the gradual increase in the Earth's temperature, contributing to 9% to 26% of the greenhouse effect [1- 4]. As a method for separating and storing CO_2, hydrate formation has attracted many researchers [5, 6]. Gas hydrates are solid crystalline substances produced by hydrogen bonding in water. Gas hydrates entrap molecules of lower molecular weight within a lattice [5]. As a unique feature, gas hydrates can hold about 180 times the gas volume [6- 9]. This high storage capacity has attracted attention to this phenomenon in the industry. In addition, the slow release of gas from hydrates, entrapment of flammable gases within the hydrates lattice and their low storage pressure are other advantages of hydrates. However, they have not been used yet in the industry due to problems such as the slow rate of hydrate formation for industrial applications, difficult separation and packaging of hydrate particles for transportation, and the presence of unreacted water within the lattice which occupies a large percentage of the volume within the hydrate lattice. Nevertheless, among the many methods of gas transmission and storage, gas hydrates can be of great interest because of their high storage capacity, the possibility of gas transfer at moderately low temperatures and at ambient pressure, easy transfer at a lower cost, and an easy production process. However, to produce them on an economic scale, one should consider problems such as high pressure and low formation rate, the need for increased stability, lower volume of gas transport compared with other methods, and water separation [10- 16]. Investigating the kinetics of hydrate formation and searching for effective promoters are very important. Several studies have been carried out on the effects of some surfactants on gas hydrate induction time, growth rate, and storage capacity [17-20]. The former method can help prepare nanofluids to improve heat and mass transfer in the hydrate formation system and provide suitable sites for heterogeneous nucleation of gas hydrates [21- 23]. The latter method can increase the solubility of the gas components in the water phase to improve their efficiency [24, 25].

In 2016, *Mohammadi et al.* examined the effect of synthesized zinc oxide (ZnO) nanoparticles on thermodynamic and kinetic equilibrium conditions of hydrate formation. The amount of gas consumption was measured and compared for four fluid samples including pure water, SDS liquid solution, water-based ZnO-nanofluid, and water-based ZnO-nanofluid in the presence of SDS (with a mass fraction of 0.001). The presence of nanoparticles resulted in a decrease in the hydrate growth time and an increase in the stored gas amount [26].

In 2016, Pivehzhani et al. investigated the optimum conditions for CO_2 hydrate formation in order to determine the maximum CO_2 storage rate and optimum energy consumption. They found that the impeller speed was the most effective factor. [27].

In 2019, *Pahlavanzadeh et al.* investigated the kinetics of methane hydrate formation in presence of SDS and CTAB as kinetic promoters. Their result indicates that SDS with a concentration of 500 ppm and CTAB with a concentration of 700 ppm are the most effective promoters in increasing the average apparent rate constant and water to hydrate conversion [28].

In 2020, *Pourranjbar et al.* studied the hydrate phase equilibria in the system containing methane gas. They used some additives such as TBAC in the presence and absence of $NaCl/MgCl_2$ in the system to figure out the hydrate formation process [29].

In 2020, *Lijun et al.* used graphene oxide and SDS as a chemical affinity model to study the kinetics of hydrate formation in different systems. According to their result, they conclude that the chemical affinity model can accurately predict the formation of hydrates in complex systems [30].

Several solutions have been proposed in this regard, and the present study addresses the use of nanoparticles and storage capacity enhancers.

EXPERIMENTAL SECTION

Materials

The carbon dioxide used for the experiments has a purity of 99.99%, which was purchased from the Arvand Industrial Gas Company. The carbon dioxide gas capsule has a volume of 20 liters and has an initial pressure of 60 bar. Tetra-N-butyl ammonium chloride, with the chemical formula $C_{16}H_{36}ClN$ and alkyl polyglycoside with a purity of 98% were purchased from Merck and Sigma-Aldrich, respectively. Alkyl Aluminum oxide nanoparticles with the purity of 99% were prepared from Nanosany product. Deionized water was also used to make the solutions. In order to stabilize the nanoparticle solution ultrasonic bath was used by the 24 kHz frequency for one hour.

Apparatus

To test, a 316-degree stainless steel jacket (SS-316) with an internal volume of 296 cm^3 which can withstand the operating pressure of 200 bar was used. The internal compartment of this reactor is equipped with four valves with a pressure tolerance of 400 bar, two of which are ball-type valves that are used to inject the solution as well as to drain the mixture of water and gas after the test and the other two valves are needle-type, one for gas injection and the other for connection to a gas chromatograph and gas sampling. In the reactor's outer wall, two holes have been created for the entry and exit of the cooling material to control the reactor temperature by passing the refrigerant. Ethylene glycol aqueous solution with a weight concentration of 50% has been used as a cooling agent and all fittings and fluid transfer pipes have been well insulated to reduce the energy loss of the reactor hydrate formation. To measure the temperature inside the reactor, a platinum temperature sensor of the Pt-100 type with an accuracy of ±0.1 K was used. The tank pressure was measured with a BD sensor with an accuracy of 0.1 bar. A swinging rotator was used to create the right mix in the main hydrate tank and a pump was used to create a vacuum inside the cell. A schematic of the hydrate formation machine used in this study is shown in Fig. 1.

Procedure

First, the reactor is washed with water by a continuous rotatory system for 10 minutes. Then it is rinsed by the distilled water. The vacuum pump is then used for 5 minutes to ensure the exit of the air and the remaining water droplets inside the reactor. 100 cm^3 aqueous solution of aluminum oxide with concentrations of 0.1 and 0.05 wt% is prepared and injected into the reactor. After setting the refrigerant temperature and stabilizing the temperature, CO_2 is injected at 40-bar initial pressure and the oscillating mixer is turned on at a fixed speed at the same time. As soon as the hydration formation process and CO_2 consumption begin, the system pressure declines. Afterward, pressure and temperature data are recorded on the computer at certain time intervals.

THEORETICAL SECTION

Amount of gas consumed

Peng-Robinson equation of state was employed for the calculation of gas consumed [31]:

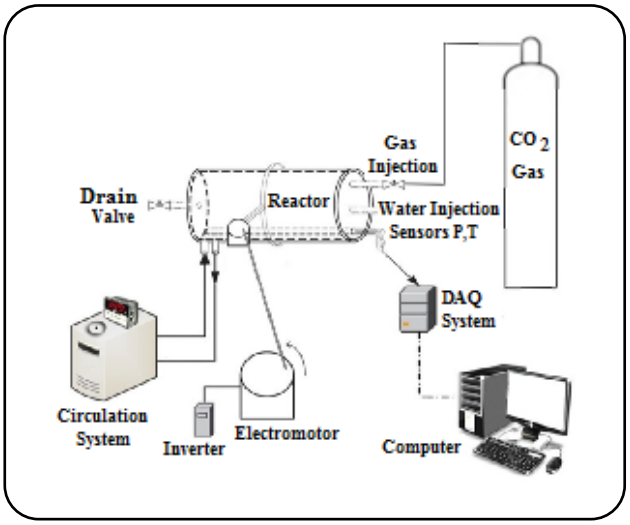

Fig. 1: Schematic of the experimental setup.

$$P = \frac{RT}{v-b} - \frac{a}{v(v+b)+b(v-b)} \quad (1)$$

Calculations should be performed by rewriting the state equation in terms of the Z compressibility coefficient. Hence, Eq. (2) is obtained with respect to Z by using the Peng-Robinson equation:

$$Z^3 - (1-B)Z^2 + (A - 2B - 3B^2)Z - (AB - B^2 - B^3) = 0 \quad (2)$$

$$A = \frac{a\alpha P}{R^2T^2} \quad (3)$$

$$B = \frac{bP}{RT} \quad (4)$$

$$a = 0.457235\frac{(RT_C)^2}{P_C} \quad (5)$$

$$b = 0.077796\frac{RT_C}{P_C} \quad (6)$$

$$\alpha = \left[1 + (m)\left(1 - (T/T_C)\right)^{0.5}\right]^2 \quad (7)$$

$$m = 0.3796 + 1.458\omega - 0.16\omega^2 + 0.01667\omega^3 \quad (8)$$

Where ν is the molar volume, T_C and P_C are temperature and pressure at the critical point, respectively, R is the universal gas constant, and ω is the acentric factor.

Using the determined Z at the initial and final pressure and temperature, the initial and final number of moles determine from Eqs. (9) and (10):

$$n_0 = \frac{P_0 V_0}{Z_0 R T_0} \quad (9)$$

$$n_e = \frac{P_e V_e}{Z_e R T_e} \quad (10)$$

$$\Delta n = n_0 - n_e \quad (11)$$

Eq. (12) is used to calculate the volume of trapped carbon dioxide at Standard Temperature and Pressure (STP) conditions.

$$V_{STP} = \frac{\Delta n R T}{P} \quad (12)$$

In Eq. (12), the volume of CO_2 gas is calculated in standard conditions (1 bar and 15 °C).

Calculation of the storage capacity

Eq. (13) was used to calculate the amount of storage capacity of carbon dioxide hydrate formation:

$$SC = \frac{V_{STP}}{V_H} = \frac{\Delta n CO_2 R T / P}{V_H} \quad (13)$$

In this equation, V_H refers to the volume of hydrate produced (which is considered here 100 cm^3).

RESULTS AND DISCUSSION

Statistical analysis of experimental results

The statistical results of the experimental data, extracted by Design expert software, are presented in Table 1. For statistical analysis, the Response surface design method and the Quadratic model have been used. In this case, five parameters affecting the carbon dioxide hydration process in water in the presence of APG surfactant, TBAC additive, and nano-particle of aluminum oxide are given to the software according to the experimental design. The parameter A is the reactor pressure. Parameter B is the reactor temperature, parameter C is the TBAC concentration, parameter D is the APG concentration and parameter E is the amount of aluminum oxide. The results of changes in the above parameters on the R1 factor of the amount of carbon dioxide storage capacity were experimentally tested and recorded. In this article, a statistical analysis of the effect of regulatory parameters on storage capacity is examined.

Statistical analysis of the parameters affecting the storage capacity of carbon dioxide in hydrates

Table 1 shows the statistical results of the effect of used additives on the storage capacity of carbon dioxide hydrate formation.

The results of ANOVA analysis are shown in Table 2.

The amounts of detection factor (R2) in Table 3, indicate that the experimental data are consistent with the predicted data. The closer number to one, the better the compliance. According to the numbers shown, good matching of the experimental data is observed.

Fig. 2 shows the experimental data versus predicted values., As shown, the data obtained are close to the 45-degree lines and are linear.

After a statistical study, a valid relationship was developed to estimate the storage capacity of carbon dioxide hydrate formation.

$$\begin{aligned} SC = {} & -1850.39290 + 182.05432(Pressure) - \\ & 8.50483(Temperature) + 43.47891(TBAC) + \\ & 0.770134(APG) + 142.51054(Al_2O_3) - \\ & 0.561901(Pressure * Temperature) - \\ & 0.859350(Pressure * TBAC) + \\ & 0.002619(Pressure * APG) - \\ & 0.664519(Pressure * Al_2O_3) \\ & -0.109602(Temperature * TBAC) - \\ & 0.003006(Temperature * APG) - \\ & 0.460133(Temperature * Al_2O_3) + \\ & 0.016776(TBAC * APG) + 3.65314(TBAC * Al_2O_3) + \\ & 0.007665(APG * Al_2O_3) - 0.343764(Pressure)^2 + \\ & 0.049547(Temperature)^2 + 0.064199(TBAC)^2 - \\ & 7.67945E-06(APG)^2 - 1.15070(Al_2O_3)^2 \end{aligned} \quad (14)$$

Fig. 3 shows the effect of initial pressure of the reactor on the storage capacity. As can be seen, the storage capacity increases with increasing pressure. Increasing the initial pressure of the reactor by increasing the driving

Table 1: Results from experimental experiments to determine storage capacity.

	Factor 1	Factor 2	Factor 3	Factor 4	Factor 5	Response 1
Run	A:Pressure	B:Temperature	C:TBAC	D:APG	E:Al_2O_3	SC
	(bar)	(k)	(Wt%)	(ppm)	(Wt%)	
1	30	279.15	1.5	500	1.5	80.8937
2	35	275.15	0	1000	0	115.73
3	30	277.15	1.5	500	1.5	81.6422
4	35	279.15	3	1000	0	122.778
5	30	275.15	1.5	500	1.5	82.0008
6	35	275.15	0	0	0	55.6734
7	35	279.15	0	1000	0	112.19
8	35	275.15	3	1000	0	127.685
9	25	275.15	3	1000	3	103.117
10	35	279.15	3	0	0	46.3071
11	25	279.15	0	1000	3	45.2167
12	30	277.15	3	500	1.5	84.1772
13	30	277.15	0	500	0	76.9489
14	35	275.15	3	0	3	50.915
15	25	275.15	3	1000	0	102.211
16	35	279.15	0	0	3	58.6723
17	35	279.15	0	0	0	38.0451
18	35	275.15	3	0	0	48.3971
19	25	277.15	1.5	500	0	47.8791
20	30	277.15	0	500	1.5	80.1137
21	30	277.15	1.5	500	3	81.9506
22	25	275.15	0	0	0	31.9124
23	35	277.15	1.5	500	1.5	96.9712
24	35	275.15	0	1000	3	118.285
25	25	277.15	1.5	500	1.5	49.8426
26	30	277.15	1.5	1000	0	99.508
27	30	279.15	1.5	500	0	77.5973
28	30	277.15	1.5	1000	3	104.285
29	30	277.15	1.5	0	1.5	59.211
30	25	279.15	3	0	0	37.0087
31	30	277.15	1.5	0	0	56.8466
32	25	275.15	3	0	0	54.412
33	30	279.15	1.5	500	3	81.322
34	25	279.15	3	1000	0	65.369
35	30	275.15	1.5	500	3	82.3023
36	30	275.15	1.5	500	0	78.5239
37	25	279.15	0	0	0	16.1444
38	35	277.15	1.5	500	0	93.003
39	30	277.15	1.5	1000	1.5	103.588
40	30	277.15	1.5	500	0	78.006
41	25	279.15	3	0	3	40.5239
42	25	279.15	0	1000	0	43.1104
43	30	277.15	3	500	0	80.8613
44	25	275.15	0	1000	0	60.4216

Table 2: ANOVA analysis results.

Source	Sum of Squares	df	Mean Square	F-value	p-value	
Model	15722.29	20	786.11	159.19	< 0.0001	significant
A-Pressure	1273.75	1	1273.75	228.75	< 0.0001	
B-Temperature	0.5986	1	0.5986	1.23	0.3301	
C-TBAC	9.83	1	9.83	1.99	0.2311	
D-APG	1129.60	1	1129.60	257.94	< 0.0001	
E-Al_2O_3	6.06	1	6.06	0.1212	0.7453	
AB	43.83	1	43.83	8.88	0.0408	
AC	58.63	1	58.63	11.87	0.0262	
AD	60.98	1	60.98	12.35	0.0246	
AE	39.84	1	39.84	8.07	0.0468	
BC	0.1501	1	0.1501	0.0304	0.8701	
BD	12.62	1	12.62	2.56	0.1851	
BE	3.52	1	3.52	0.7131	0.4460	
CD	225.24	1	225.24	45.61	0.0025	
CE	108.37	1	108.37	21.95	0.0094	
DE	54.38	1	54.38	11.01	0.0294	
A^2	197.49	1	197.49	39.99	0.0032	
B^2	0.1235	1	0.1235	0.0250	0.8820	
C^2	0.0558	1	0.0558	0.0113	0.9205	
D^2	11.32	1	11.32	2.29	0.2045	
E^2	19.75	1	19.75	4.00	0.1161	
Residual	19.75	4	4.94			
Cor Total	15742.05	24				

Table 3: Statistical table of answers.

Std. Dev.	2.22	R^2	0.9987
Mean	77.86	Adjusted R^2	0.9925
C.V. %	2.85	Predicted R^2	0.8375
		Adeq Precision	47.0175

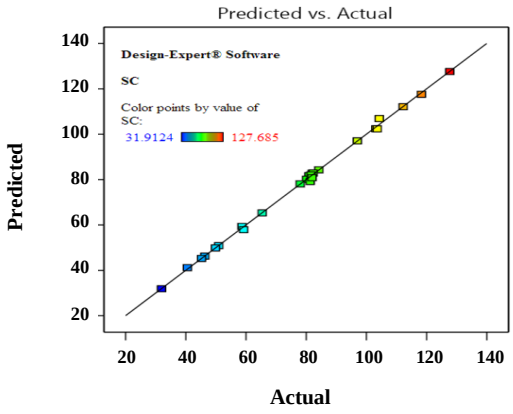

Fig. 2: Real chart values versus predicted values.

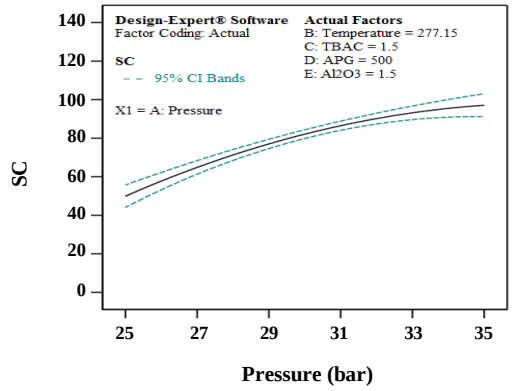

Fig. 3: The change of the storage capacity of carbon dioxide in hydrate with reactor pressure.

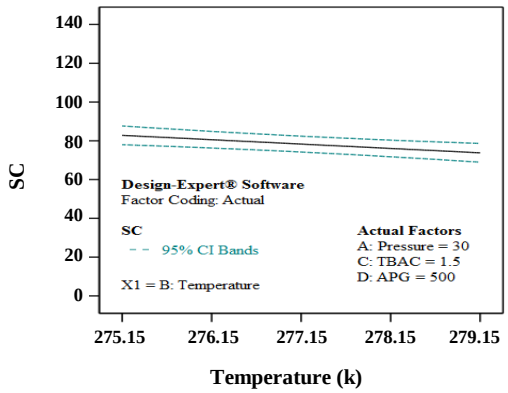

Fig. 4: The change of the storage capacity of carbon dioxide in hydrated at temperature.

the force of carbon dioxide hydrate formation, increases the amount of storage capacity.

Fig. 4 shows the effect of the temperature on the storage capacity of carbon dioxide hydrate formation. As can be seen, as the temperature rises, the storage capacity of carbon dioxide in the hydrate decreases. This is due to the negative effect of increasing the temperature on the driving force of hydrate formation.

Fig. 5 shows the effect of various concentrations of TBAC on the storage capacity of carbon dioxide hydrate formation. As can be seen, by increasing the concentrations of TBAC from 0 to 3 wt%, the storage capacity of carbon dioxide hydrate increases. TBAC is a thermodynamic promoter of hydrate formation and utilization of this additive by moderating the thermodynamic conditions of carbon dioxide hydrate formation increases the driving force and therefore increases the storage capacity of carbon dioxide hydrate formation.

Fig. 6 shows how to change the storage capacity of carbon dioxide in hydrate with APG concentration. As can be seen, with increasing APG concentration, the storage capacity of carbon dioxide in the hydrate increases sharply. One of the effects of adding APG is a drastic reduction in surface tension between water and gas. By reducing the surface tension, the gas penetration resistance in water and hydrate is significantly reduced.

Fig. 7 shows how the Al_2O_3 concentration of carbon dioxide storage capacity changes in hydrate with concentration (aluminum oxide). As can be seen, with the conditions defined for this experiment, with increasing Al_2O_3 concentration, the storage capacity of carbon dioxide in the hydrate does not change much and is slightly increasing. At the temperature and pressure of the hydrate formation cavities produced by hydrogen bonding in water, some of these cavities are occupied by aluminum oxide and as a result, the penetration of carbon dioxide into the hydrate is reduced and the storage capacity is slightly increased.

In Figs. 3 to 7 of the single effect, the parameters affecting the storage capacity of carbon dioxide in the hydrate (regardless of the interaction between them) are analyzed. Due to Figs. 3 to 7 and statistical Relations (14), the addition of APG has had the greatest impact on storage capacity. Figs. 8 to 13 examine the interaction between effective parameters.

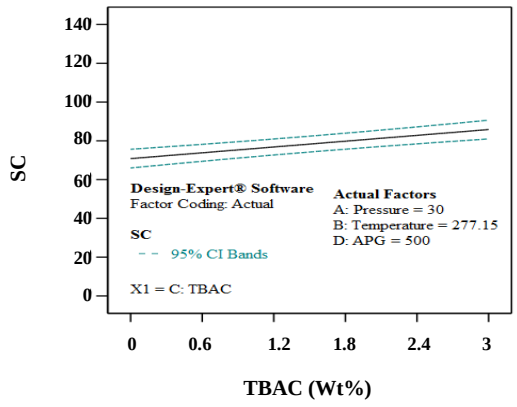

Fig. 5: The change of the storage capacity of carbon dioxide in hydrate with TBAC.

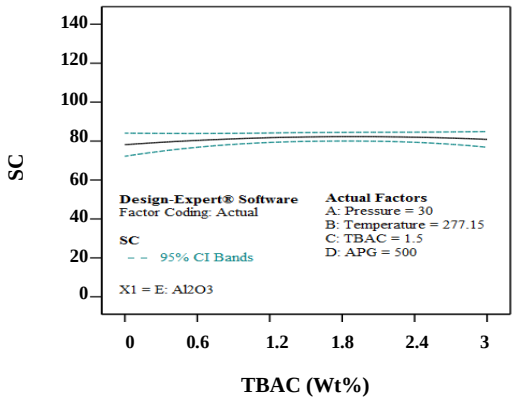

Fig. 7: The change of the storage capacity of carbon dioxide in hydrate with Al_2O_3 concentration.

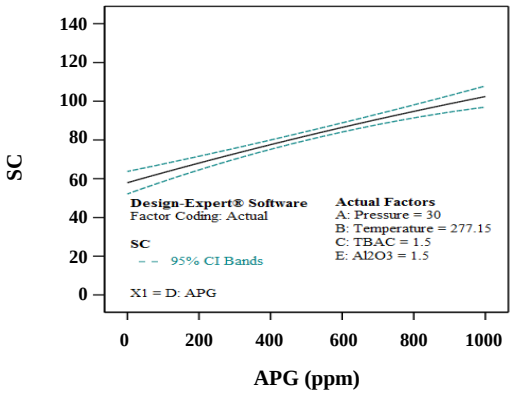

Fig. 6: The change of the storage capacity of carbon dioxide absorption in hydrates with APG concentration.

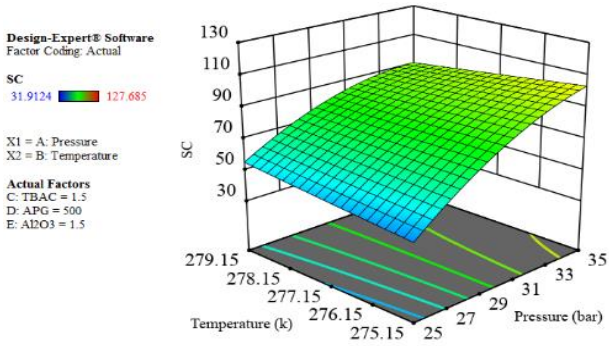

Fig. 8: The effect of simultaneous interaction of pressure and temperature parameters of the reactor on the storage capacity of carbon dioxide in the hydrate.

As can be seen in Fig. 8, the simultaneous effect of temperature and pressure on the storage capacity of carbon dioxide can be said to be much lower than the pressure change.

Fig. 9 also shows the simultaneous effect of pressure and APG on the three-dimensional diagram. It is observed that at high pressures as well as at high concentrations of APG, the storage capacity of carbon dioxide hydrate is in the best conditions. Because the lowest amount of storage capacity is when we see the amount of pressure and APG and vice versa.

Fig. 10 shows the interaction of pressure and concentration of aluminum oxide on the storage capacity of carbon dioxide in the hydrate.

As shown in Fig. 11, low-temperature conditions as well as high APG concentrations. Also the amount of carbon dioxide hydrate storage capacity is really optimal.

Fig. 12 also shows that there is no significant interaction between the parameters of temperature and concentration of aluminum oxide under the experimental conditions in the storage capacity of carbon dioxide hydrate.

Fig. 13 also shows the interaction between the APG and Al_2O_3 concentration parameters. At high concentrations of APG and Al_2O_3, the storage capacity of carbon dioxide hydrate is observed to increase.

The behavior of the APG and TBAC concentration parameters on the carbon dioxide storage capacity in Fig. 14 is the same as the simultaneous effect of pressure and APG.

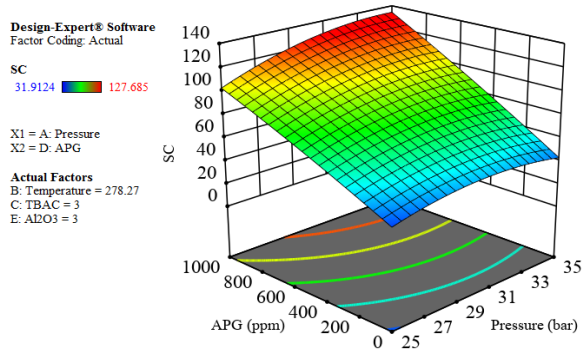

Fig. 9: Effect of simultaneous action of pressure parameters and APG concentration on carbon dioxide storage capacity in hydrate.

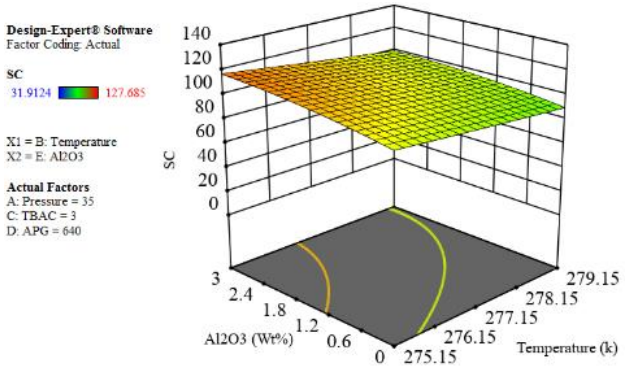

Fig. 12: The effect of simultaneous interaction of temperature parameters and Al_2O_3 concentration on the storage capacity of carbon dioxide in the hydrate.

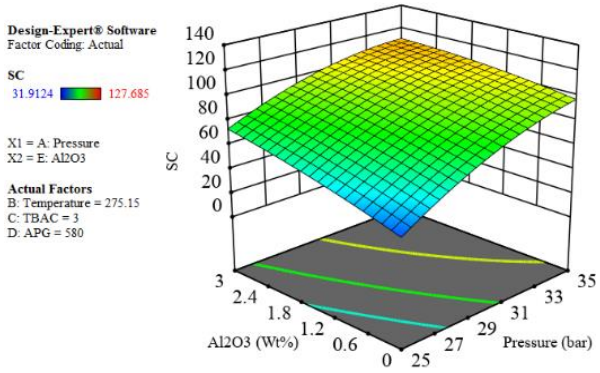

Fig. 10: The effect of simultaneous interaction of pressure and concentration parameters of Al_2O_3 on the storage capacity of carbon dioxide in the hydrate.

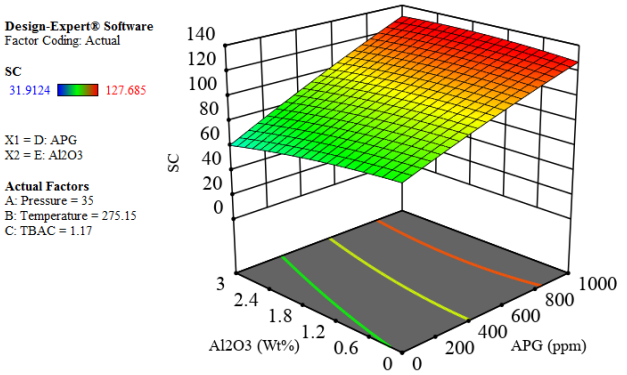

Fig. 13: Simultaneous interaction of APG and Al_2O_3 concentration parameters on the amount of carbon dioxide storage capacity in the hydrate.

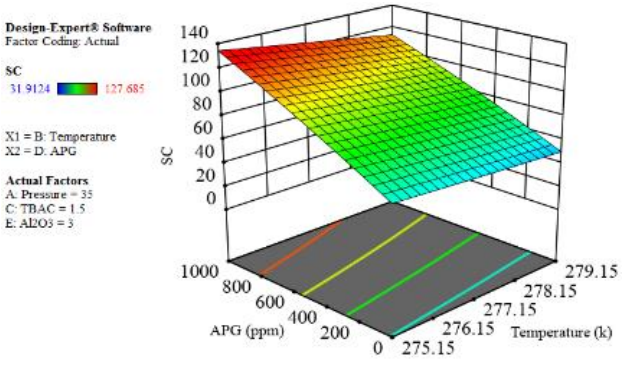

Fig. 11: The effect of simultaneous action of temperature parameters and APG concentration on the storage capacity of carbon dioxide in the hydrate.

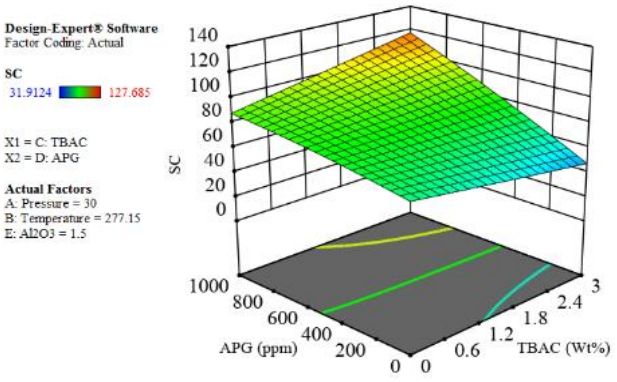

Fig. 14: Simultaneous interaction of APG and TBAC concentration parameters on the amount of carbon dioxide storage capacity in the hydrate.

Table 4: Optimal laboratory conditions for maximum storage capacity.

Pressure	Temperature	TBAC	APG	Al_2O_3	SC	Desirability	
34.558	276.085	2.825	956.733	2.436	137.476	1.000	Selected

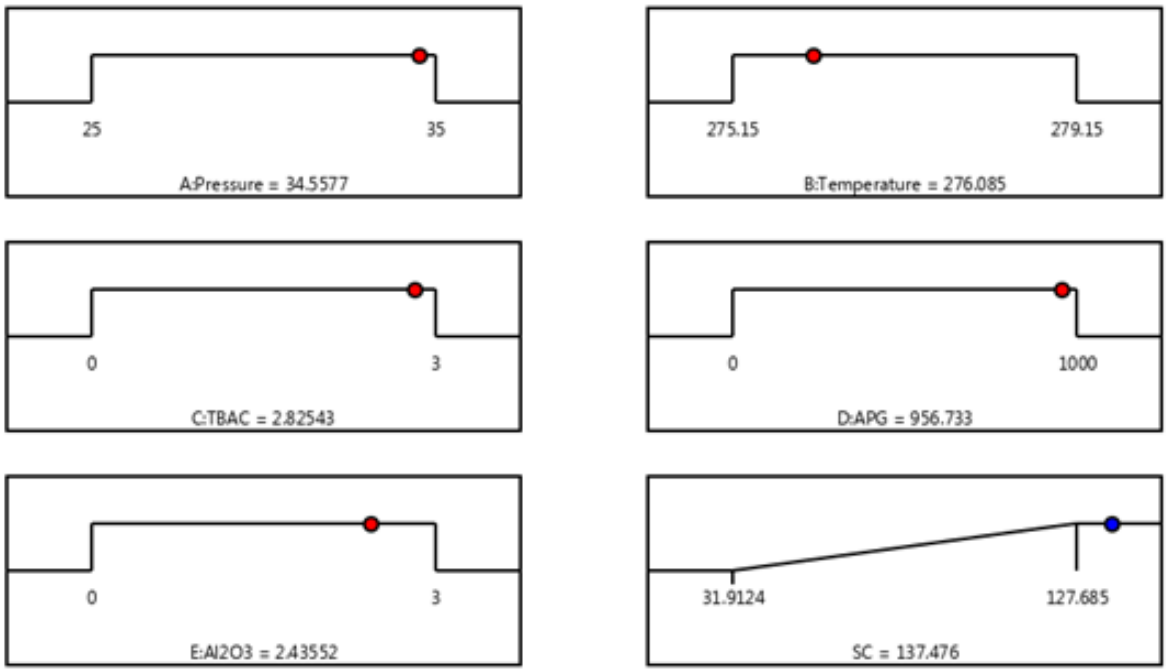

Fig. 15: Sloping surface diagram in optimal condition.

It is observed that in high concentrations of APG and TBAC, the storage capacity of carbon dioxide hydrate is in the best conditions and the most ideal distribution. Because the maximum amount of storage capacity is in the case where we see the maximum amount of TBAC and APG and vice versa.

Optimization conditions

The results of optimizing the amount of storage capacity using the software are shown below. It should be noted that Table 4 of the optimal laboratory conditions for the maximum amount of storage capacity is stated.

In the following, we can also check the sloping surface diagram. The sloping surface will be as follows in the maximum amount of storage capacity (Fig. 13).

The points marked in Fig. 15 in the variables range expressed, indicate the optimal point which is the maximum storage capacity of carbon dioxide gas.

CONCLUSIONS

In the present study, statistical analysis of carbon dioxide gas storage capacity in hydrate was conducted in the presence of alkyl polyglycoside surfactant (APG), aluminum nanoparticle oxide, and Tetra-Butyl Ammonium Vhloride (TBAC) additive. The impact factor of the parameters was statistically presented by a mathematical relationship with $R^2 = 0.9987$ to estimate the CO_2 storage capacity in hydrates. The results showed that adding APG to the system at constant temperature and pressure increases the storage capacity by 75% while adding 5% aluminum oxide nanoparticles and TBAC 38% increased storage capacity. Also, the simultaneous effect of the parameters was doubled on the storage capacity which was most affected by the high concentration APG with the increase of each pressure parameter and the TBAC concentration and the most optimal mode which is the maximum storage capacity of carbon dioxide is in high concentrations of APG, TBAC, and high pressure and low temperature.

Nomenclature

P	Pressure
P_0	Initial gas pressure based on bar
P_e	Equilibrium (final) gas pressure based on bar
P_c	Critical pressure
T	Temperature
T_c	Critical temperature
T_0	Initial gas temperature based on STP
T_e	Final gas temperature based on STP
Z	Compressibility factor
Z_0	Gas compressibility coefficient at an initial pressure and temperature
Z_e	Gas compressibility coefficient at final pressure and temperature
V	Volume of the gas phase
V_0	Initial gas volume based on cm^3
V_e	Final gas volume based on cm^3
υ	Molar volume
n_0	Initial number of moles
n_e	Final number of moles
A, B, a, α, b and m	Constants
ω	Acentric factor
R	Universal gas constant 83.14 $(bar.cm^3)/(mol.K)$
SC	Storage Capacity
V_H	Hydrate formation volume based on cm^3

Acknowledgments

The authors of the paper thank the direct financial and spiritual support provided by the head of the University and deputy of research and technology of Marvdasht of Islamic Azad University, sincerely.

Received : Jun 28, 2020 ; Accepted :Sep. 28, 2020

REFERENCES

[1] Bozorgian A., Arab Aboosadi Z., Mohammadi A., Honarvar B., Azimi A., Optimization of Determination of CO_2 Gas Hydrates Surface Tension in the Presence of Non-Ionic Surfactants and TBAC, *Eurasian Chem. Commun.*, **2(3)**: 420-426 (2020).

[2] Bozorgian A., Samimi A., A Review of Kinetics of Hydrate Formation and the Mechanism of the Effect of the Inhibitors on It, *Int. J. New Chem.*, [Articles in Press], (2020).

[3] Bozorgian, A., Arab Aboosadi, Z., Mohammadi, A., Honarvar, B. Azimi, A., Evaluation of the Effect of Nonionic Surfactants and TBAC on Surface Tension of CO2 Gas Hydrate, *J. Chem. Pet. Eng.*, **54(1)**: 73-81 (2020).

[4] Bozorgian A., Arab Aboosadi Z., Mohammadi A., Honarvar B., Azimi A., Prediction of Gas Hydrate Formation in Industries, *Prog. Chem. Biochem. Res.*, **3(1)**:31-38 (2020).

[5] Mashhadizadeh J, Bozorgian A, Azimi A., Investigation of the Kinetics of Formation of Clatrit-Like Dual Hydrates TBAC in the Presence of CTAB, *Eurasian Chem. Commun.*, **2(4)**: 536-47 (2019).

[6] Shi L., Liang D., Investigation of Kinetics of Tetrabutylammonium Chloride (TBAC) + CH_4 Semiclathrate Hydrate Formation, *RSC Adv*; **7**: 53563-53569 (2017).

[7] Yang M., Song Y., Jiang L., Liu Y., Li Y., CO_2 Hydrate Formation Characteristics in a Water/Brine-Saturated Silica Gel, *Ind. Eng. Chem. Res*; **53(26)**: 10753-10761(2014).

[8] Zang X., Lv Q., Li X., Li G., Experimental Investigation on Cyclopentane–Methane Hydrate Formation Kinetics in Brine, *Energy & Fuels*, **31(1)**: 824-883 (2017).

[9] Liu R., Gao F., Liang K., Yuan Z., Ruan Ch., Wang L., Yang Sh., Experimental Study on the Correlation Between Rapid Formation of Gas Hydrate and Diffusion of Guest Molecules, *Appl. Therm. Eng.* , **154**: 393-399 (2019).

[10] Yan Sh., Dai W., Wang Sh., Rao Y., Zhou Sh., Graphene Oxide: An Effective Promoter for CO_2 Hydrate Formation, *Energies*, 11**(7)**: 1756 (2018).

[11] Wang P., Zhou H., Ling Z., Li Y., Hydrate Formation Characteristics during Carbon Dioxide Flow Through Depleted Methane Hydrate Deposits, *Energy Technology*, **6(6)**: 1186-1195 (2018).

[12] Babaee S., Hashemi H., Mohammadi A.H., Naidoo P., Ramjugernath D., Experimental Measurement and Thermodynamic Modelling of Hydrate Phase Equilibrium Conditions for Krypton + N-Butyl Ammonium Bromide Aqueous Solution, *J. Supercrit. Fluids*, **107**: 676-681 (2016).

[13] Veluswamy H.P., Kumar A., Seo Y., Lee J., Linga P., A Review of Solidified Natural Gas (SNG) Technology for Gas Storage *via* Clathrate Hydrates, *Appl. Energy*, **216**: 262-285 (2018).

[14] Wang Y., Lang X., Fan Sh., Hydrate Capture CO_2 From Shifted Synthesis Gas, Flue Gas and Sour Natural Gas or Biogas, *J. Energy Chem.*, **22(1)**: 39-47 (2013).

[15] Moeini H., Bonyadi M., Esmaeilzadeh F., Rasoolzadeh A., Experimental Study pf Sodium Chloride Aqueous Solution Effect on the Kinetic Parameters of Carbon Dioxide Hydrate Formation in the Presence/Absence of Magnetic Field, *J. Nat. Gas Sci. Eng.* , **50**: 231-239 (2018).

[16] Babaee S., Hashemi H., Mohammadi A.H., Naidoo P., Ramjugernath D., Kinetic Study of Hydrate Formation for Argon + TBAB + SDS Aqueous Solution System, *J. Chem. Thermodynamics*, **116**: 121–129 (2018).

[17] Ganji H., Manteghian M., Omidkhah M., Mofrad H.R., Effect of Different Surfactants on Methane Hydrate Formation Rate, Stability and Storage Capacity, *Fuel*, **86(3)**: 434–441(2007).

[18] Ganji H., Manteghian M., Mofrad H.R., Effect of Mixed Compounds on Methane Hydrate Formation and Dissociation Rates and Storage Capacity, *Fuel Process. Technol.*, **88(9)**: 891–895 (2007).

[19] Zhang J., Lee S., Lee J.W., Kinetics of Methane Hydrate Formation from SDS Solution, *Ind. Eng. Chem. Res*., **46(19)**:6353–9635 (2007).

[20] Karimi R., Varaminian F., Izadpanah A.A., Mohammadi A.H., Effects of Different Surfactants on the Kinetics of Ethane-Hydrate Formation: Experimental and Modeling Studies, *Energy Technol.*, **1(9)**:530–536 (2013).

[21] Yu Y.S., Zhou S.D., Li X.S., Wang S.L., Effect of Graphite Nanoparticles on CO_2 Hydrate Phase Equilibrium, *Fluid Phase Equilib.*, **414**: 23-28 (2016).

[22] Mohammadi Khoshraj B., Seyyed Najafi F., Mohammadi Khoshraj J., Ranjbar H., Microencapsulation of Butyl Palmitate in Polystyrene-co-Methyl Methacrylate Shell for Thermal Energy Storage Application, *Iran. J. Chem. Chem. Eng. (IJCCE)*, **87**: 187-194 (2018).

[23] Henriques Delicia C., Wigent R., Effect of Adding Potassium Chloride on Tetra-n-butyl Ammonium Chloride Semiclathrate Thermal Stability at Atmospheric Pressure, *J. Chem. Eng. Data*, **64(12)**: 5946–5958 (2019).

[24] Yu Y.S., Zhou Sh., Li X., Wang Sh., Effect of Graphite Nanoparticles on CO2 Hydrate Phase Equilibrium, *Fluid Phase Equilib.*, **414**: 23-28 (2016).

[25] A. Mohammadi, M. Manteghian, A. Haghtalab, A.H. Mohammadi, M. Rahmati-Abkenar, Kinetic Study of Carbon Dioxide Hydrate Formation in Presence of Silver Nanoparticles and SDS, *Chem. Eng. J.*, **237**: 387–395 (2014).

[26] Mohammadi M., Haghtalab A., Fakhroueian Z., Experimental Study and Thermodynamic Modeling of CO_2 Gas Hydrate Formation in Presence of Zinc oxide Nanoparticles, *J. Chem. Thermodynamics*, **96**: 24 –33 (2016).

[27] Pivezhani F., Roosta H., Dashti A., Mazloumi H., Investigation of CO_2 Hydrate Formation Conditions for Determining the Optimum CO_2 Storage Rate and Energy: Modeling and Experimental Study, *Energy*, **113**: 215-226 (2016).

[28] Pahlavanzadeha H., Khanlarkhania M., Rezaeia S., Mohammadi A.M., Experimental and Modelling Studies on the Effects of Nanofluids (SiO_2, Al_2O_3, and CuO) and Surfactants (SDS and CTAB) on CH_4 and CO_2 Clathrate Hydrates Formation, *Fuel*, **253:** 1392-1405 (2019).

[29] Pourranjbar M., Pahlavanzadeh H., Askari Zadeh Mahani A., Mohammadi A.M., Hydrate Phase Equilibria of Methane + TBAC + Water System in the Presence and Absence of NaCl and/or $MgCl_2$, *J. Chem. Eng. Data*, Articles in Press, (2020).

[30] Li L., Zhao Sh., Wang Sh., Rao Y., CO2 Hydrate Formation Kinetics Based on a Chemical Affinity Model in the Presence of GO and SDS, *RSC Adv.*, **10**: 12451-12459 (2020).

[31] Mohammadpour A., Mirzaei M., Azimi A., Tabatabaei Ghomsheh S.M., Solubility and Absorption Rate of CO_2 in MEA in the Presence of Graphene Oxide Nanoparticle and Sodium Dodecyl Sulfate, *Int. J. Ind. Chem.*, **10**: 205–212 (2019).